Biointerphases
A Journal of Biomaterials and Biological Interfaces

Injectable biocompatible poly(2-oxazoline) hydrogels by strain promoted alkyne–azide cycloaddition

Cite as: Biointerphases **16**, 011001 (2021); https://doi.org/10.1116/6.0000630
Submitted: 14 September 2020 • Accepted: 09 December 2020 • Published Online: 05 January 2021

Jong-Ryul Park, Eleonore C. L. Bolle, Amanda Dos Santos Cavalcanti, et al.

Biointerphases
A Journal of Biomaterials and Biological Interfaces

ARTICLE

avs.scitation.org/journal/bip

Injectable biocompatible poly(2-oxazoline) hydrogels by strain promoted alkyne–azide cycloaddition

Cite as: Biointerphases 16, 011001 (2021); doi: 10.1116/6.0000630
Submitted: 14 September 2020 · Accepted: 9 December 2020 ·
Published Online: 5 January 2021

Jong-Ryul Park,[1] Eleonore C. L. Bolle,[1] Amanda Dos Santos Cavalcanti,[1] Annelore Podevyn,[2] Joachim F. R. Van Guyse,[2] Aurelien Forget,[3] Richard Hoogenboom,[2,a)] and Tim R. Dargaville[1,b)]

AFFILIATIONS

[1]Institute of Health and Biomedical Innovation, Science and Engineering Faculty, Queensland University of Technology, Brisbane, QLD 4001, Australia
[2]Supramolecular Chemistry Group, Centre of Macromolecular Chemistry (CMaC), Department of Organic and Macromolecular Chemistry, Ghent University, Krijgslaan 281 S4, B-9000 Ghent, Belgium
[3]Institute for Macromolecular Chemistry, University of Freiburg, Stefan-Meier-St. 31, Freiburg, 79104, Germany

Note: This paper is part of the Biointerphases Special Topic Collection on Biointerface Science in Australia 2020 - An issue in celebration of Hans Griesser's career.

[a)]**Electronic mail:** Richard.Hoogenboom@UGent.be
[b)]**Electronic mail:** t.dargaville@qut.edu.au

ABSTRACT

Poly(2-alkyl-2-oxazoline) (PAOx) hydrogels are tailorable synthetic materials with demonstrated biomedical applications, thanks to their excellent biocompatibility and tunable properties. However, their use as injectable hydrogels is challenging as it requires invasive surgical procedures to insert the formed hydrogel into the body due to their nonsoluble 3D network structures. Herein, we introduce cyclooctyne and azide functional side chains to poly(2-oxazoline) copolymers to induce *in situ* gelation using strain promoted alkyne–azide cycloaddition. The gelation occurs rapidly, within 5 min, under physiological conditions when two polymer solutions are simply mixed. The influence of several parameters, such as temperature and different aqueous solutions, and stoichiometric ratios between the two polymers on the structural properties of the resultant hydrogels have been investigated. The gel formation within tissue samples was verified by subcutaneous injection of the polymer solution into an *ex vivo* model. The degradation study of the hydrogels *in vitro* showed that the degradation rate was highly dependent on the type of media, ranging from days to a month. This result opens up the potential uses of PAOx hydrogels in attempts to achieve optimal, injectable drug delivery systems and tissue engineering.

I. INTRODUCTION

Poly(2-alkyl-2-oxazoline) (PAOx) hydrogels have been explored as platforms for biomedical applications, such as tissue engineering[1,2] and drug delivery systems.[3–5] Thanks to the advances in well-controlled polymerization of PAOx with unprecedented levels of tailorable properties,[6–8] fine-tuning of hydrogels is feasible with various crosslinking chemistries.[9–14] To date, crosslinking chemistry to fabricate PAOx hydrogels has been beset with drawbacks due to the presence of potentially toxic additives (such as initiators,[10,12] crosslinkers,[11] catalysts,[15] and enzymes[16]) or external stimuli (such as heating[13,17] or UV light[3]) to initiate gelation. The lack of biocompatible crosslinking limits the use of PAOx hydrogels for biomedical applications as these hydrogels have to form before implantation. Using these hydrogels in a clinical setup requires invasive surgery to insert the preformed hydrogels into the body, which adds complexity to its implementation. Designing a biocompatible *in situ* crosslinking system for PAOx would allow overcoming these issues and enable their use as injectable hydrogels.

Injectable hydrogels could be prepared as two-part polymer solutions that are injected into the targeted area *via* a dual syringe,

which eliminates the need for invasive surgery.[18] In addition, these hydrogels could be designed to be directly delivered to an inaccessible site by key-hole surgery.[19]

To date, only a few studies have reported the use of injectable PAOx hydrogels based on physical/ionic interaction, leading to physically crosslinked hydrogels.[20–22] Such hydrogels are limited by the need for making substantial changes to the environmental conditions to trigger gelation (e.g., heat or pH change), often leading to a slow sol–gel transition. Besides, physical interactions to build networks are usually not stable *in vivo* due to the sensitivity of the noncovalent bonds to external conditions such as change of temperature or ionic strength.[23] On the other hand, injectable hydrogels with covalent crosslinks have several advantages such as its rapid gelation, long-term stability, and better mechanical properties.

Several crosslinking strategies to achieve *in situ* forming hydrogels with diverse synthetic polymers have been proposed, including but not limited to Diels–Alder cycloaddition,[24,25] hydrazone formation,[26–28] thiol-Michael addition,[29,30] and copper-catalyzed alkyne–azide cycloaddition.[31] Using these chemistries, copolymers with 2-*n*-(pent-4′-ynyl)-2-oxazoline could be a candidate for preparing *in situ* forming PAOx hydrogels under mild conditions. For example, the alkyne group containing PAOx has already been widely used with various azide compounds to manipulate polymer properties[32,33] to incorporate drugs,[15] crosslinkers, and to synthesize cyclic polymers.[34] However, this click reaction possesses a limitation due to the presence of a copper(I) catalyst, leading to low efficiency and damaging the tissue *in vivo*, which is not an ideal way to achieve injectable hydrogels.[35]

Herein, we demonstrate that strain promoted alkyne–azide cycloaddition (SPAAC) is a promising tool to make injectable PAOx hydrogels since this reaction does not require any toxic catalyst or external stimuli.[36,37] For example, Hodgson *et al.* synthesized injectable polyethylene glycol (PEG) hydrogels *via* SPAAC and reported very rapid gelation (≤2 min) without any external stimuli and catalyst, and the synthesized hydrogels were nontoxic.[38,39] Also, SPAAC has already been successfully used for bioconjugation, proving its biocompatibility,[40–44] and this reaction is bio-orthogonal, and, thus, it avoids undesired reactions with biomolecules. For instance, Madl *et al.* proved the bio-orthogonality of SPAAC by showing further reactions of functional groups in hydrogels after cell encapsulation.[45] The 2-alkyl-2-oxazoline monomer, 2-methoxycarbonyl-alkyl-2-oxazoline (MestOx), was identified as a candidate to introduce functionalities for SPAAC chemistry due to its effective amidation process with a variety of functional groups.[46] Particularly, the resulting amidated PAOx is relatively hydrophilic due to the presence of a secondary amide group in the side chain, making it a promising precursor to introduce cyclooctyne and azide functional groups and to produce the injectable hydrogels.

Here, we synthesized and characterized two PAOx hydrogel precursors, one possessing azide moieties in the side chain, named PAOx-Azide, and the complementary aryl-less cyclooctyne (ALO) containing PAOx, named PAOx-ALO. These PAOx derivatives were designed with an ester moiety in the side chain to ensure biodegradability through ester hydrolysis. The precursors, PAOx-Azide and PAOx-ALO, were used to fabricate the injectable PAOx hydrogels *via* SPAAC click chemistry. The results demonstrated that the formation of biocompatible PAOx hydrogels could be carried out within biological tissue by simply mixing two polymer solutions. A wide range of hydrogel properties could be controlled by various conditions, such as polymer concentration, temperature, media, and stoichiometric precursor ratios for the desired biomedical applications.

II. MATERIALS AND METHODS

A. Materials

The following chemicals were used as received: glutaric anhydride (>98%, TCI chemicals), thionyl chloride ($SOCl_2$) (>98%, Merck), 2-chloroethylamine hydrochloride (98%, Acros Organics), aminoethanol (98%, TCI chemicals), 1,5,7-triazabicyclo[4.4.0] dec-5-ene (TBD) (98%, Merck), ethyl-4-bromobutanoate (95%, Merck), sodium azide (≥99.5%, Merck), cycloheptene (97%, Merck), methyl glycolate (98%, Merck), potassium *tert*-butoxide (98%, Merck), bromoform (99%, Merck), silver triflate (≥99%, Merck), 4-(dimethylamino)pyridine (DMAP) (≥99%, Merck), and *N*-(3-dimethylaminopropyl)-*N*′-ethylcarbodiimide (EDC) (98%, Merck). The monomer, 2-ethyl-2-oxazoline (EtOx) (a gift from Polymer Chemistry Innovations, USA) was dried over barium oxide (BaO) before use. Methyl *p*-toluenesulfonate (MeOTs) was chosen as the initiator and used after distillation. Acetonitrile (ACN) was purified by using a solvent purification system (J. C. Meyer), and water was purified using a Sartorius arium® pro system.

B. Characterization

1D ^{1}H NMR spectra were recorded using an Avance 600 MHz Bruker spectrometer using $CDCl_3$ or DMSO as a solvent. Size-exclusion chromatography (SEC) was measured on an Agilent 1260-series high-performance liquid chromatography system equipped with an inline degasser, a diode array detector, a refractive index detector, and a temperature controller set to 50 °C. The mobile phase was *N*,*N*′-dimethylacetamide (DMAc) with 0.8% lithium bromide (LiBr) at a flow rate of 0.5 ml/min. Poly(methyl methacrylate) standards from Polymer Standards Service were used to determine the average molar mass and dispersity (*Đ*). Mass spectroscopy was recorded using gas-phase ion–molecule experiments performed on a linear quadrupole ion trap mass spectrometer (LTQ XL, Thermo Fisher Scientific, San Jose, CA) with a heated electrospray ionization source. The sample in methanol was prepared at the concentration of 1 mM and eluted into the source at the rate of 25 μl/min. Mass analysis was set to scan a 100–500 mass rage in negative ionization mode.

C. Rheological behavior

Rheological properties of the hydrogels were investigated using an Antron Parr M302 rheometer with the 25 mm plate (top) and quartz plate (bottom) geometry. After mixing two solutions containing two polymers, the solution was placed on the plate of the rheometer. After 2 min, time sweep was conducted to monitor the storage modulus (G′) and the loss modulus (G″) in the process of hydrogel formation with a frequency of 1 rad/s, a strain of 1%, and a 0.06 mm gap. After the final storage modulus of the hydrogels was obtained, the frequency sweep test was investigated with the frequency ranging from 1 to 1000 rad/s.

D. Swelling and *in vitro* degradation study

Hydrogel swelling ratios were measured by a gravimetric method. The hydrogels were dried under reduced pressure at 25 °C until constant weights were obtained. The dried hydrogels were immersed in phosphate-buffered saline (PBS) (*p*H of 7.4) at 37 °C, and the masses of swollen hydrogels were measured at incubation times of 6 and 72 h. Here, the swelling ratio is defined as swelling ratio = $(W_s - W_d)/W_d$, where W_s is the weight of the hydrogels after swelling in PBS buffer and W_d is the weight of dry hydrogels. *In vitro* degradation of the hydrogels was studied by monitoring the swelling ratio of the hydrogels periodically. The swollen hydrogels were incubated in four different aqueous solutions, PBS (*p*H of 7.4), PBS with the presence of sodium hydroxide (*p*H of 8.5), PBS with the presence of hydrochloric acid (*p*H of 6.0), and human blood serum (a gift from the Translational Research Institute, Brisbane, Australia).

E. *Ex vivo* forming gelation and histology

The two polymer solutions with 100 μl of solutions containing 10 mg of PAOx-Azide and 100 μl containing 10 mg of PAOx-ALO were mixed using a vortex machine, and the mixture was injected by subcutaneous injection into an *ex vivo* model [cadaver of a C57BL/6 mouse (Queensland University of Technology Research Ethics Committee 1900000716)] at room temperature. After an hour's incubation, the samples were collected and fixed in 4% paraformaldehyde for 24 h followed by PBS washing and incubation in 70% (v/v) ethanol until further analysis. The specimens were dehydrated with a graded ethanol series in an automated Excelsior ES tissue processor (Thermo Fisher Scientific, Waltham, USA) and embedded in paraffin. Then, 5-mm thickness sections were obtained and stained with hematoxylin and eosin using a Leica ST5010XL autostainer.

F. Cell viability

1. Fibroblast isolation

Human primary fibroblasts were isolated from consenting patients undergoing elective surgery,[47] following methods published by Xie *et al.*[47] and Haridas *et al.*[48] Ethical approval for fibroblast isolation was obtained from the Queensland University of Technology Research Ethics Committee (No. 1300000063) and the

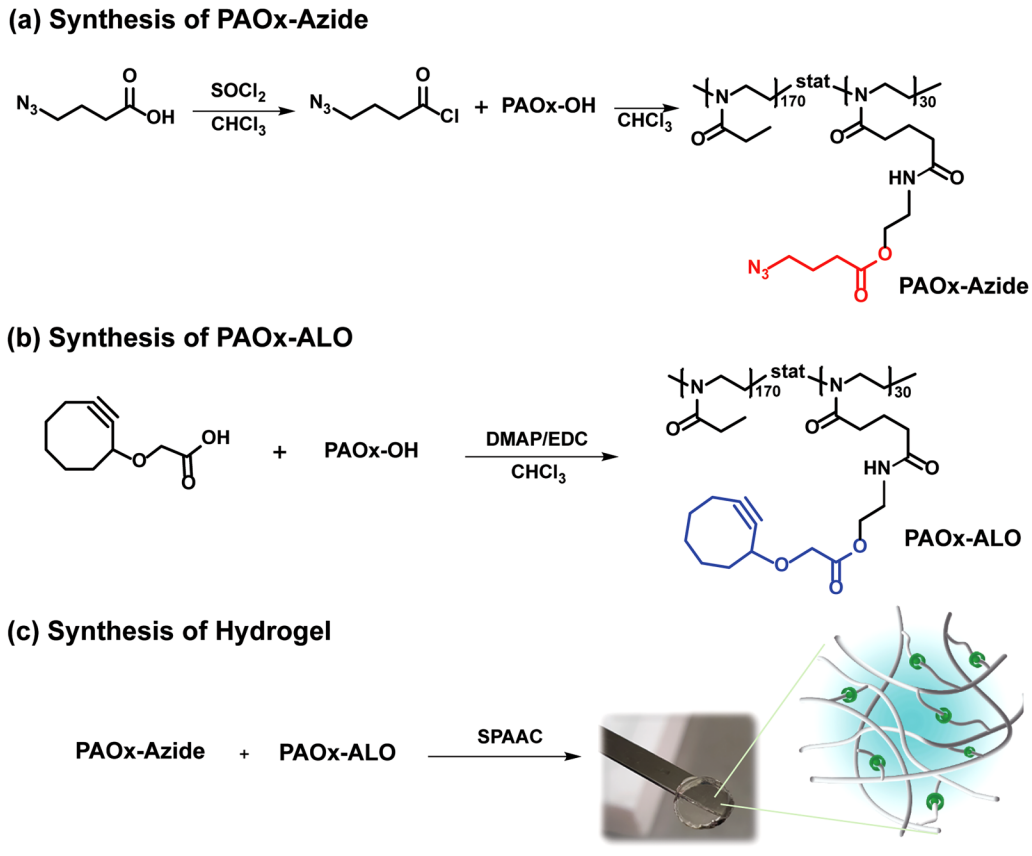

FIG. 1. Synthetic routes for the preparation of (a) PAOx-Azide and (b) PAOx-ALO and (b) strain promoted alkyne–azide cycloaddition reaction of two polymers to yield PAOx hydrogels.

Uniting Healthcare/St Andrew's Hospital Ethics Committee (No. 0346). Cells were cultured in Dulbecco's modified Eagle's medium (DMEM) supplemented with 10%(v/v) fetal bovine serum and 1%(v/v) penicillin and streptomycin. Cells at P4 were used upon reaching 90% confluency.

2. Cytotoxicity of polymer compounds on fibroblasts

Polymer stock solutions were prepared in a sterile fibroblast medium at 10% w/v. Different polymer dilutions were then prepared by further diluting the stock solution with the fibroblast medium. In total, seven different concentrations were tested: 0.1, 0.2, 2, 5, 10, 15, and 20 mg/ml. Each dilution was tested in triplicate. Fibroblasts were plated in 96 well plates at a density of 2000 cells per well. Following an overnight incubation, to allow for cell attachment, the culture medium was removed and replaced with 100 μl of polymer dilutions. The cells were then incubated in the presence of the polymer for another 24 h, and upon reaching this timepoint, WST-1 reagent (Merck, Australia) at a concentration of 100 ml/ml was added to the samples and incubated for another 4 h, according to the manufacturer's protocol. Absorbance was measured on a microplate reader at a wavelength of 450 nm with the reference wavelength set to 650 nm. Cells cultured in a standard fibroblast medium without polymer served as a positive control, and cell viability was calculated as percent change to the positive control.

3. Cell morphology in the presence of hydrogels

Cell morphology of the fibroblasts cultured in the presence of PAOx hydrogels was also evaluated. The hydrogels were sterilized in 70% v/v ethanol overnight and then, rinsed in PBS (4 × 1 h), prior to submerging in serum-free DMEM for 4 h. Cells at P3 were used for this experiment. Each hydrogel was seeded with 10 μl of DMEM containing 30 000 cells and incubated for 1 h before the addition of 2 ml of the fibroblast

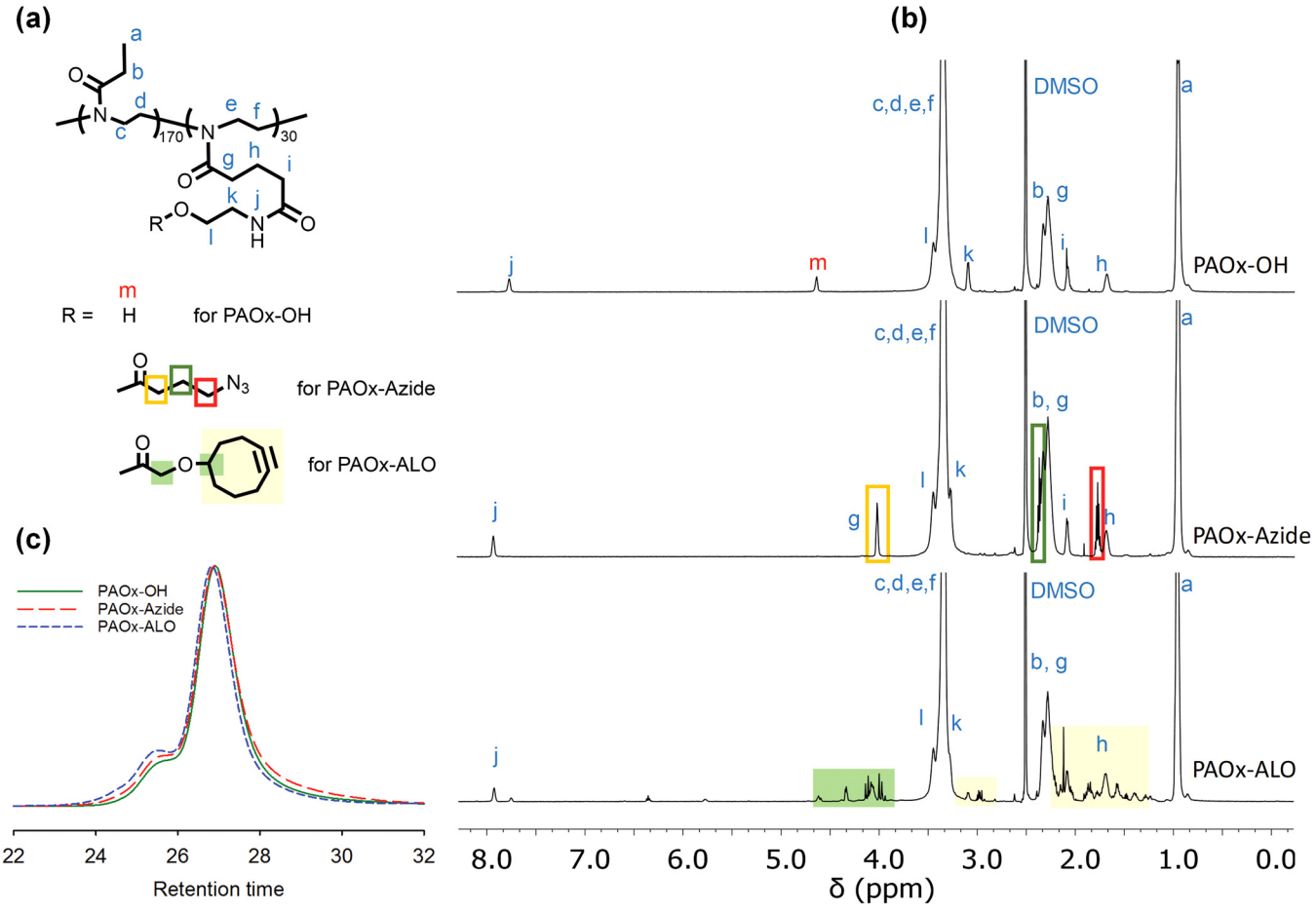

FIG. 2. (a) Chemical structures of polymers, (b) ^{1}H NMR spectra in DMSO-d_6, and (c) the normalized RI SEC traces of PAOx-OH, PAOx-Azide, and PAOx-ALO with DMAc with 0.8% lithium bromide as the eluent.

medium. Cells cultured on tissue culture treated well plates served as the control. The cells were cultured for 48 h. After 48 h, the cells were rinsed in PBS, supplemented with Ca^{2+} and Mg^{2+}, and then fixed in 4% paraformaldehyde overnight at 4 °C. Following fixation, the cells were permeabilized in Triton X-100 (0.2% v/v) for 5 min and then incubated in a 1% w/v bovine serum albumin blocking solution for 5 min. The cells were fluorescently labeled with 4′,6-diamidino-2-phenylindole (DAPI) and Phalloidin by placing them in a working solution containing a blocking solution, 0.8 U/ml TRITC Phalloidin, and 5 μg/ml DAPI for 45 min, protected from light, on an orbital shaker. Samples were washed three times in PBS between steps and imaged on an epifluorescence microscope (Eclipse Ti-S, Nikon, Japan).

III. SYNTHETIC PROCEDURES

A. Polymerizations

Polymerizations were carried out by cationic ring-opening polymerization (CROP). A solution containing EtOx (5.05 g, 0.051 mol, 170 eq.), 2-methoxycarbonyl-propyl-2-oxazoline (C_3MestOx) (1.54 g, 0.009 mol, 30 eq.), MeOTs (45 ml, 0.3 mmol, 1 eq.), and 8.5 ml of ACN was prepared in a glovebox with a water and oxygen concentration ≤0.1 ppm, and the polymerization mixture was reacted at 140 °C in a microwave synthesizer (Biotage initiator$^+$) for 28 min. Consecutively, TBD (0.63 g, 4.5 mmol, 0.5 eq. to C_3MestOx) and 2-aminoethanol (3.3 ml, 54 mmol, 6 eq. to C_3MestOx) were added to the mixture and reacted at 170 °C for 9 min to yield hydroxyl functionalized PAOx (PAOx-OH). The polymer was precipitated in cold diethyl ether, and the obtained polymer was purified by dialysis against distilled water for 3 days and dried in a freeze dryer. ^{1}H NMR (600 MHz, DMSO-d_6) [Fig. 1(b)]: 7.75 [m, 25H, NH(C═O)], 4.62 (m, 25H, OH), 3.66-3.15 [m, 850H, NCH_2CH_2 and CH (C═O)], 3.09 (m, 50H, CH_2NH), 2.41-2.14 [m, 390H, CH_2(C═O)], 2.16-2.00 [m, 50H, CH_2(C═O)], 1.76-1.59 (m, 50H, CH_2), 1.06 (m, 510H, CH_3). M_n (SEC) = 21.4 kDa, $Đ$ (SEC) = 1.24, recovery mass = 82.6%.

B. Incorporation of functional groups

The synthetic routes for the preparation of cyclooct-1-yn-3-glycolic acid (aryl-less cyclooctyn, ALO) and 4-azidobutanoic acid are included in the supporting information (Schemes S1 and S2).[61] As shown in Scheme 1(a) and 1(b), the two functionalized PAOx were synthesized by esterification in different manners, as described below.

1. Synthesis of PAOx-Azide

Excess thionyl chloride was added dropwise to the solution of 4-azidobutanoic acid (0.26 g, 2.04 mmol, 1.5 eq. of relative to the hydroxyl group of PAOx) in 3 ml of chloroform at room temperature, and the mixture was reacted for 3 h. After thionyl chloride and chloroform were removed under vacuum, the resulting 4-azidobutanoic acid chloride was dissolved in a small portion of chloroform, and the solution was added to the PAOx-OH (1.0 g, 0.045 mmol) solution in 5 ml of chloroform. After the reaction was stirred overnight, the polymer was precipitated in cold diethyl ether, purified by dialysis against distilled water for 48 h, and dried in a freeze dryer. ^{1}H NMR (600 MHz, DMSO-d_6) [Fig. 1(b)]: 5.73 (m, 31H, $CHCH_2$), 4.89 (m, 62H, $CHCH_2$), 3.73-3.12 (m, 800H, NCH_2CH_2), 2.31 (m, 60H, CHCH═CH_2), 2.14-1.90 [s, m, 570H, CH_3 and (C═O)CH_2], 1.5 (m, 60H, CH_2), 1.37-1.10 (m, 300H, CH_2). M_n (SEC) = 20.6 kDa, $Đ$ (SEC) = 1.31, recovery mass = 87.2%.

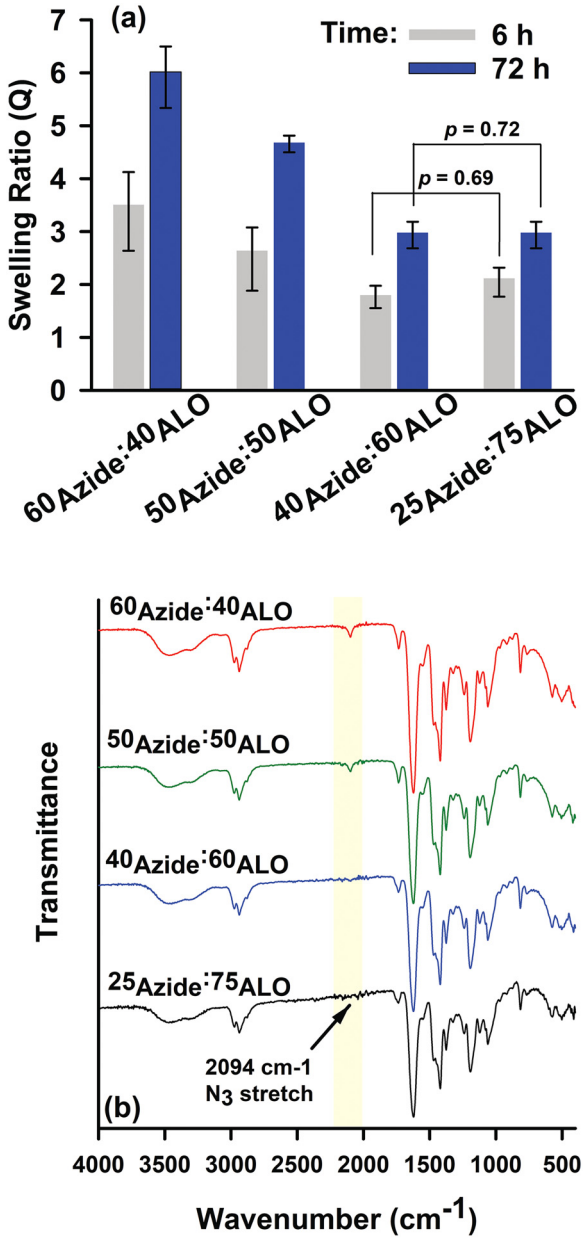

FIG. 3. (a) Swelling ratio [Mean ± standard error (n = 3)] and (b) FTIR spectra of hydrogels with different ratios of PAOx-ALO and PAOx-Azide.

2. Synthesis of PAOx-ALO

Cyclooct-1-yn-3-glycolic acid (0.06 g, 0.34 mmol, 1.1 eq. of hydroxyl group of PAOx), PAOx-OH (0.2 g, 0.01 mmol), EDC (0.066 g, 0.35 mmol), and DMAP (0.043 g, 0.35 mmol) were dissolved in dichloromethane, and the mixture was reacted overnight. The polymer was precipitated in diethyl ether and purified by dialysis against distilled water for 48 h and dried in a freeze dryer. ^{1}H NMR (600 MHz, DMSO-d_6) [Fig. 1(b)]: 5.73 (m, 31H, $CHCH_2$), 4.89 (m, 62H, $CHCH_2$), 3.73-3.12 (m, 800H, NCH_2CH_2), 2.31 (m, 60H, $CHCH{=}CH_2$), 2.14-1.90 [s, m, 570H, CH_3 and $(C{=}O)CH_2$], 1.5 (m, 60H, CH_2), 1.37-1.10 (m, 300H, CH_2). M_n (SEC) = 25.2 kDa, $Đ$ (SEC) = 1.19, recovery mass = 84.5%.

3. Hydrogel preparation

Hydrogels were fabricated by mixing the two polymers, PAOx-Azide and PAOx-ALO, and dissolved in PBS with 10 wt. % concentration. After mixing the two polymer solutions using a vortex machine, the resulting mixtures (60 μl) were pipetted onto the Teflon mold and compressed with coverslips suspended on 1 mm spacers to form discs, followed by incubation at 37 °C for 20 min.

IV. RESULTS AND DISCUSSION

A. Synthesis of PAOx-OH

The monomer, C_3MestOx, is particularly useful in synthesizing functional PAOx copolymers as it enables the incorporation of methyl-ester groups into the side chains that are easily transformed into a wide variety of other functional groups through amidation.[46] As MestOx is not commercially available, it was synthesized by a modified Wenker method,[49] as shown in Scheme S3 in the supplementary material.[61] Subsequently, MestOx was copolymerized with EtOx using a monomer to initiator ratio of [EtOx]:[C_3MestOx]:[MeOTs] = 170:30:1. The CROP resulted in high conversions (>95% by gas chromatography) after heating for 28 min at 140 °C (Scheme S4 in the supplementary material).[61] The methyl-ester groups of the resulting PEtOx-C_3MestOx copolymer were amidated by TBD-catalyzed amidation[50] (Scheme S4 in the supplementary material)[61] using a sixfold excess of 2-aminoethanol in such a way that quantitative conversion of the methyl ester was achieved to yield the hydroxyl functionalized PAOx copolymer (PAOx-OH).

PAOx-OH was successfully synthesized using an experimental molecular weight (21.4 kg/mol) that was in good agreement with the theoretical molar mass (25.8 kg/mol) and a relatively low dispersity ($Đ$ = 1.24). The completed amidation was evidenced by the disappearance of the ester group at 1730 cm^{-1} in the FTIR

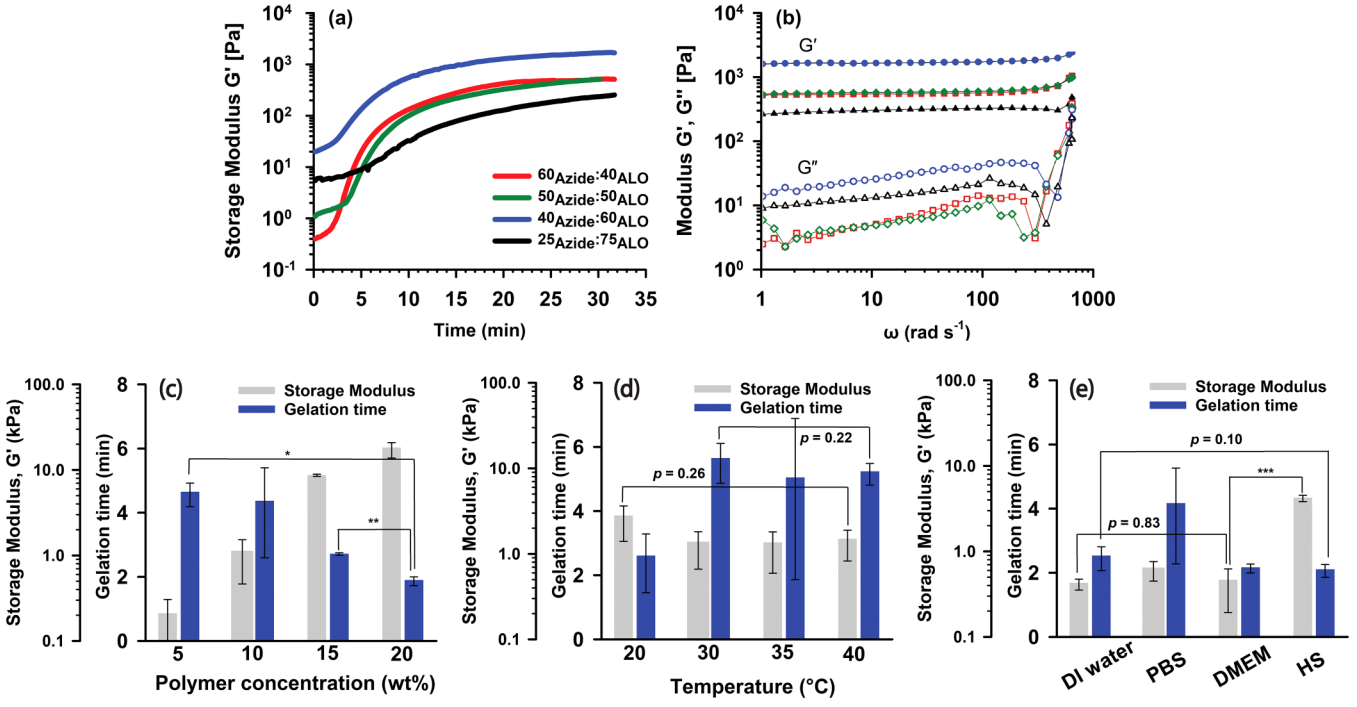

FIG. 4. (a) Storage modulus and (b) frequency sweep dynamic analysis of the hydrogels with a different ratio of two precursors, dependency of the gelation time and storage modulus on (c) polymer concentrations with the fixed temperature (37 °C) and media (PBS, *p*H = 7.4), (d) temperatures with the fixed media (PBS, *p*H = 7.4) and 10 wt. % polymer concentration, and (e) media with the temperature (37 °C) and 10 wt. % polymer concentration. Mean ± standard error (n = 3), DI water = distilled water; PBS = phosphate-buffered saline; DMEM = Dulbecco's modified Eagle's medium, and HS = human blood serum. *p < 0.05, **p < 0.005, and ***p < 0.0005 statistical analysis by one-way analysis of variance.

spectrum (Fig. S1 in the supplementary material)[61] assigned to the methyl-ester group of C_3MestOx.[51] The amidation was further confirmed by ^{1}H NMR spectroscopy showing the presence of an amide peak [(C═O)NH] at 7.8 ppm and a hydroxyl peak at 4.6 ppm [Fig. 2(b)]. The resulting PAOx-OH had a calculated hydroxyl group content of 14 mol. %, which was in good agreement with the targeted degree of modification of 15 mol. %.

B. Incorporation of functional groups

Two functional groups for the SPAAC reaction having a carboxylic acid group for conjugation to PAOx-OH, namely, cyclooct-1-yn-3-glycolic acid (ALO) and 4-azidobutanoic acid, were synthesized according to Burk *et al.*[52] and Reux *et al.*[53] ^{1}H NMR spectra (Fig. S2 in the supplementary material)[61] and mass spectroscopy [Figs. S3(a) and S3(b) in the supplementary material][61] revealed the successful syntheses of both the 4-azidobutanoic acid (m/z = 128.0 + H) and cyclooct-1-yn-3-glycolic acid (m/z = 181 + H). To further confirm the structures and their reactivity, the two compounds were mixed in ethanol, resulting in the SPAAC formation of a triazole compound with the correct molar mass (m/z = 310.3 + H) [Fig. S3(c) in the supplementary material].[61]

As depicted in Fig. 1(a), the synthesis of PAOx-Azide was achieved by the reaction between PAOx-OH and 4-azidobutanoic acid chloride that was prepared with thionyl chloride. In the case of PAOx-ALO, a DMAP-meditated ester coupling reaction was used to conjugate ALO to PAOx-OH due to the suspected instability of cyclooctyne in the presence of hydrochloride that is released in the thionyl chloride reaction. In Fig. 2(b), the ^{1}H NMR spectrum of PAOx-Azide is shown, indicating the successful coupling of 4-azidobutanoic acid and ALO to PAOx-OH. The functionalization degree of the polymers was determined by ^{1}H NMR spectroscopy by comparing the peak integration between the methyl group of PEtOx at 1.0 ppm and the adjacent methylene group at 4.0 ppm for azide conjugation and 4.3 ppm for ALO conjugation. All hydroxyl groups of PAOx-OH were converted to azide or ALO, leading to 14 mol. % functionalization degree. The FTIR spectra in Fig. S4 in the supplementary material[61] confirmed the successful synthesis of the two polymers, showing the presence of the ester group at 1730 cm^{-1}. The SEC results are shown in Fig. 2(c), revealing an increase in molar mass when the functional groups were attached to PAOx-OH, which is a further indication of the successful functionalization of PAOx. An increase of the shoulder at high molar mass was observed, probably due to minor coupling reactions derived from ester-exchange reactions or heterogeneous functionality of the starting polymer.

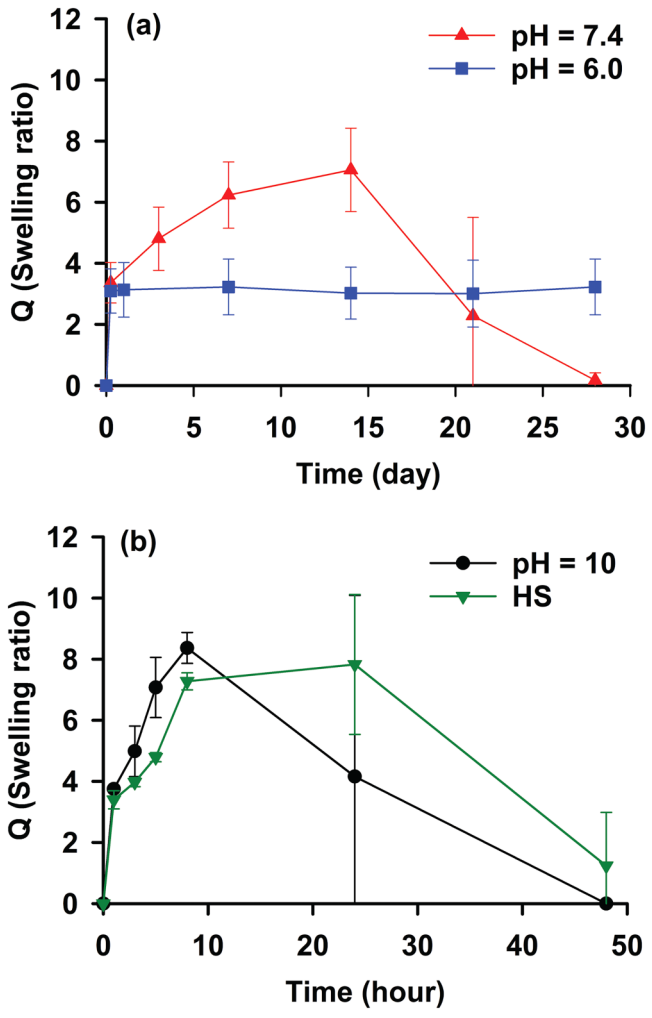

FIG. 5. (a) *In vitro* degradation studies of hydrogels with composition of 40% PAOx-Azide and 60% PAOx-ALO in four different aqueous solutions. (a) *p*H = 7.4 and 6.0 (b) *p*H = 10 and human blood serum. Incubation temperature = 37 °C. Mean ± standard error (n = 3).

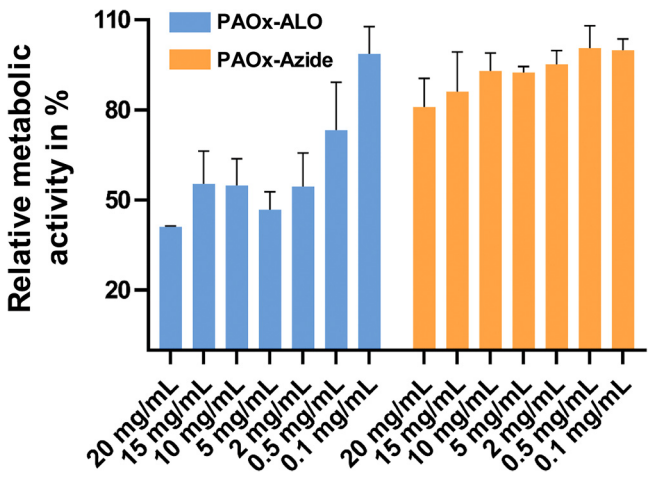

FIG. 6. Cell metabolic activity of human dermal fibroblasts cultured in the presence of PAOx-Azide and PAOx-ALO with various concentrations for 24 h at 37 °C.

C. Hydrogel formation and swelling ratio

The preparation of PAOx hydrogels was achieved by simply mixing two stock solutions containing PAOx-Azide and PAOx-ALO in PBS (pH = 7.4). The hydrogels were prepared with four different ratios between PAOx-Azide and PAOx-ALO solutions while maintaining a constant polymer concentration of 10 wt. %. The formation of hydrogels was successful with all compositions yielding colorless and transparent PAOx hydrogels with gel fractions >98 wt. % (where the gel fraction is 100× the dry mass after crosslinking/precursor mass). The swelling ratio of the hydrogels with different ratios of the two precursor polymers in PBS (pH = 7.4) is shown in Fig. 3(a). The hydrogel with a precursor ratio of 40% PAOx-Azide and 60% PAOx-ALO showed the lowest swelling ratio among the four compositions, meaning that the hydrogel with this composition consists of the highest crosslinking density. When the same amounts of both polymers were used, the residual azide functional group at 2097 cm^{-1} was observed in the FTIR spectrum, indicating that not all azide groups were consumed during the hydrogel formation, which could be due to either ALO-homocoupling or the inaccessibility of ALO- and/or azide groups [Fig. 3(b)]. Interestingly, the swelling ratio of hydrogels with 25% PAOx-Azide and 75% PAOx-ALO was the same as that for the hydrogel with 40% PAOx-Azide and 60% PAOx-ALO with a p-value of 0.69 for a 6 h incubation and a p-value of 0.72 for a 72 h incubation, despite the expected lower crosslinking density. This unexpected result is attributed to the hydrophobicity of ALO, which could lead to a reduction in hydrogel swelling.[54,55]

D. Rheological behavior

Dynamic time sweep rheological experiments were carried out to monitor the gelation time, storage modulus (G′), and loss modulus (G″) of PAOx hydrogels under various conditions. Here, the time to the apparent gel point was taken as the crossover in G′ and G″. In Fig. 4(a), the G′ of the PAOx hydrogels with the various ratios of the two polymer solutions in PBS (pH = 7.4) indicated that the hydrogel with a ratio of 40% PAOx-Azide and 60% PAOx-ALO showed the highest final G′ values of 1.4 ± 0.2 kPa resulting in stiffer gels, which was in agreement with its lowest swelling degree that indicated the highest crosslink density. The PAOx hydrogels with other compositions revealed a G′ value of 0.4 ± 0.15 kPa. Furthermore, the gelation time of the hydrogel with the ratio of 40% PAOx-Azide and 60% PAOx-ALO was the fastest (Fig. S5 in the supplementary material).[61] As expected, the hydrogel with the ratio of 25% of PAOx-Azide and 75% PAOx-ALO is softer than the other compositions, meaning that it has the lowest crosslinking density.

In Fig. 4(b), frequency sweep dynamic analysis revealed the energy storage or dissipation of hydrogels as a function of strain.

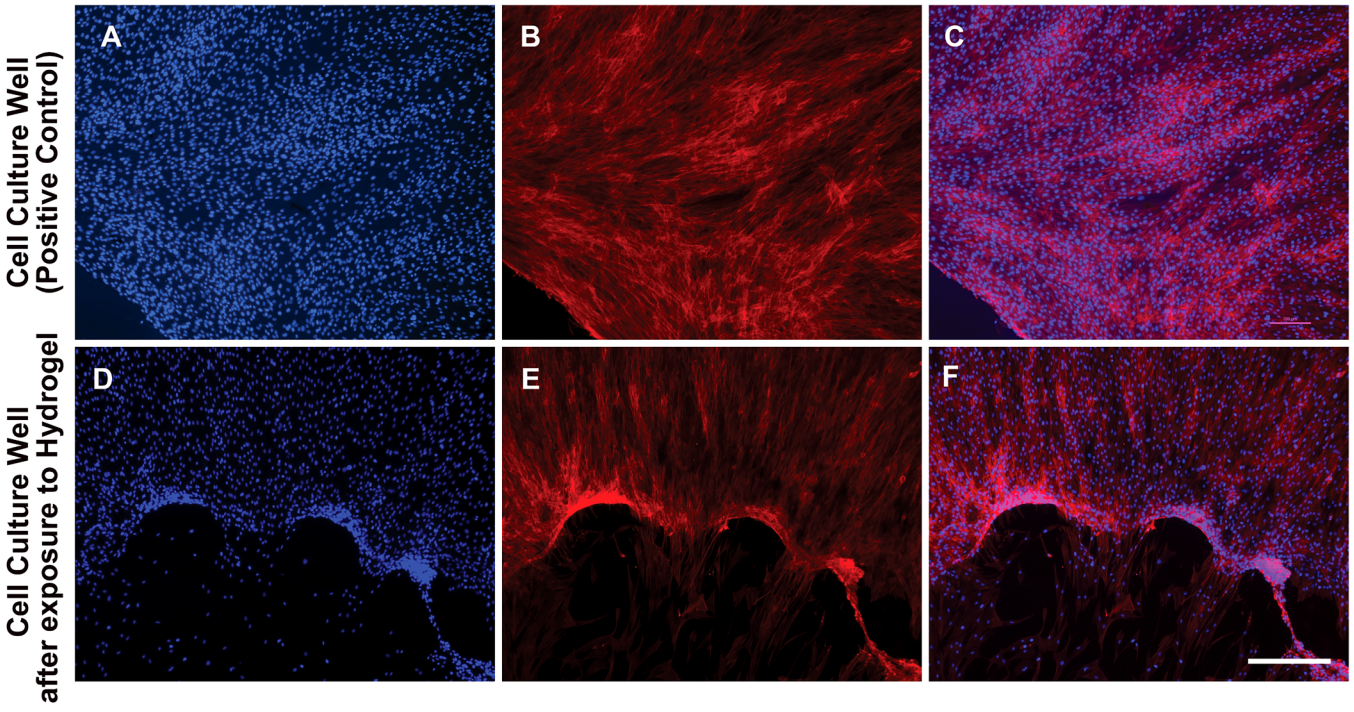

FIG. 7. Representative microscope images of fibroblasts cultured in the presence of the hydrogels. Top row [(a)–(C)] is the tissue culture plastic control, and the bottom row [(d)–(F)] is the tissue culture plastic after the removal of a PAOx-ALO/PAOx-Azide hydrogel. Cell nuclei were stained with DAPI [(a) and (d)], and the cell cytoskeleton was stained with Phalloidin [(b) and (e)] and merged [(c) and (f)]. The dark regions in (d)–(F) are where the hydrogel was before removal and staining. The scale bar denotes 400 μm.

Of note, G′ and G″ of the hydrogels have a low dependence on the frequency in a range from 1 to 100 rad/s, which was expected for chemically crosslinked hydrogels. Beyond the frequency range at 100 rad/s, both G′ and G″ noticeably increased since the elasticity of hydrogels is dependent on the polymer concentration in water, also including the presence of imperfections (e.g., dangling ends of polymer, chain entanglements, or uncross-linked polymer chains).[32] The average loss factors of the hydrogels with all compositions were near zero ($>4.4 \times 10^{-2}$), meaning that the energy proportion stored elastically in the hydrogels was high compared with energy dissipation.[56] Rheological behavior was further investigated with different polymer concentrations, temperatures, and aqueous solutions, as shown in Figs. 4(c)–4(e). The gelation time and G′ could be tuned by the control of polymer concentration in the medium (Fig. S6 in the supplementary material).[61] The results show that 5 wt. % polymer solution could not form a gel (G′ = 4.3 Pa after 30 min at 37 °C), suggesting that this concentration is below the limit of network formation. At high polymer concentration, the storage modulus of the hydrogels was comparatively high up to 18 kPa and showed a rapid gelation time down to 2 min for 20 wt. % polymer concentration. As depicted in Figs. 4(d) and 4(e), the rheological behavior of the hydrogels showed the effect of temperatures and aqueous solvents. The gelation at 20 °C was slightly faster due to perhaps the higher solubility of polymers at a lower temperature. However, little statistical difference ($p = 0.26$) on storage modulus was observed among the four different temperatures, meaning that the gelation of the two polymers was insensitive to external stimuli to initiate gelation (Fig. S7 in the supplementary material).[61] Moreover, the statistical difference in G′ for the hydrogels obtained in distilled water, PBS, and DMEM (serum-free media) was negligible (p-value = 0.83). However, interestingly, a significant increase in G′ ($p < 0.0001$) was observed in the hydrogel with human blood serum compared with other hydrogels obtained from the other three aqueous solutions.

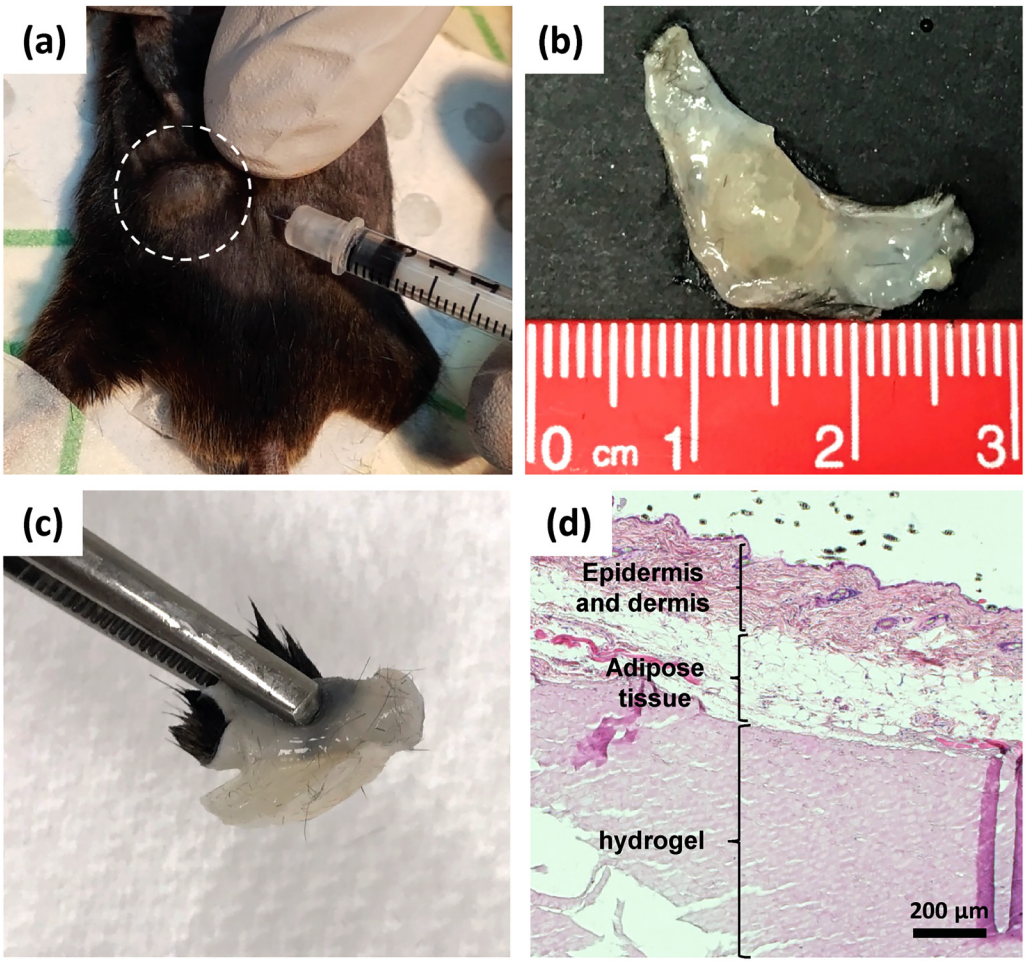

FIG. 8. (a) Picture of the injection of the polymer solutions (injection volume = 200 µl, a composition of 50% PAOx-Azide, and 50% PAOx-ALO) and (b) and (c) excised hydrogel formed in subcutaneous tissue. (d) Hematoxylin and eosin staining of a cross section of the tissue containing the PAOx hydrogel.

This observation may be explained by an interaction between albumin contained in serum (the albumin concentration is known as 35–50 mg/ml in human blood serum[57]) and the PAOx gels, or an increase of macromolecular density from the proteins present in human blood serum.

E. Hydrogel degradation

In vitro degradation of the hydrogels (5 ± 0.5 mg in dry weight with a composition of 60% PAOx-Azide and 40% PAOx-ALO) was carried out based on the swelling ratio (Fig. 5). The degradation of the hydrogels was studied at four different *p*H aqueous solutions (*p*H = 6.0, 7.3, and 10) and human blood serum. The degradability of the hydrogels has a strong dependence on the type of aqueous solutions. The swelling ratio of hydrogels in PBS (*p*H = 7.4) [Fig. 5(a)] gradually increased within 15 days due to a decrease in crosslinking density, ascribed to ester hydrolysis. Subsequently, swelling ratios dramatically decreased as the hydrogels disintegrated and eventually completely dissolved over a month. However, hydrogels at a *p*H of 6 were relatively stable with a constant swelling ratio that increased very slowly by time. This is expected because the ester linkage is associated with high stability under a mildly acidic environment.[58] On the other hand, the swelling ratio of the hydrogels in the solution with a *p*H of 10 and human serum degraded much quickly within 2–3 days [Fig. 5(b)]. It is considered that the difference in the degradability of the hydrogels was affected by the kinetics of degradation of the ester linkage, especially, for human blood serum contained enzymes for ester and amide hydrolysis.[59,60]

F. Cell viability

Cellular metabolic activity in the presence of PAOx-ALO and PAOx-Azide was measured using the WST-1 assay (Fig. 6). Cells cultured in the presence of PAOx-Azide had high metabolic activity (above 80%) for all tested concentrations. Cells cultured in the presence of PAOx-ALO showed a trend toward decreasing cell viability with an increasing polymer concentration. This result indicates the importance of determining the cytotoxicity of novel PAOx derivatives. Nonetheless, we expect that the *in situ* forming PAOx hydrogel based on PAOx-ALO and PAOx-Azide will be biocompatible as the ALO groups will be embedded in the PAOx matrix. Therefore, the cell behavior was investigated in the presence of the hydrogels. Figure 7 shows representative images of the cell culture plate following removal of the hydrogels. The cells exhibited an elongated morphology, typical of that observed in fibroblasts cultured *in vitro*. This suggests that the synthesized hydrogels are nontoxic to surrounding cells *in vitro*.

G. *Ex vivo* hydrogel formation

To investigate the *in situ* formation of PAOx hydrogels, a 200 μl mixture of two polymer solutions containing 10 mg of PAOx-Azide and 10 mg of PAOx-ALO, which easily flowed through a 29G needle (0.184 mm inner diameter), was injected subcutaneously into an *ex vivo* mouse model, resulting in a localized swollen hydrogel in the injection site [Fig. 8(a) highlighted]. The hydrogels were successfully formed *in situ* and were collected from the excised tissue an hour after injection [Figs. 8(b) and 8(c)]. The hydrogel was found to adhere to the tissue sample [Fig. 8(b)] and needed a force to be detached from the skin tissue. Even though we attempted to measure the adhesion force between the tissue and the hydrogel, the force could not be detected using our current experimental methods (a universal testing machine with a 5 N load cell). The observed adhesion could be explained by the hydrophobic interaction of ALO or produced triazole with tissue samples and may be beneficial for the fixation of the hydrogel suppressing its migration post injection. Histological analysis confirmed the presence of the hydrogel near the injection area in the subcutaneous tissue of the mouse [Fig. 8(d)], and a microscopic image of the boundary between the resultant hydrogel and adipose tissue sample indicated good integration.

V. CONCLUSIONS

This work introduced biocompatible, injectable, and degradable poly(2-oxazoline) hydrogels *via* SPAAC chemistry. The hydrogel properties such as the swelling ratio, storage/loss modulus, and gelation time for ideal PAOx hydrogels can be tuned by varying the concentration of the aqueous solution of polymers. The *p*H of the incubation solution controls the degradation time of PAOx hydrogels, which is related to ester hydrolysis. We expect that the current work will facilitate the design of PAOx hydrogels to achieve novel drug delivery devices or tissue engineering scaffolds via *in situ* forming crosslinks.

ACKNOWLEDGMENTS

T.R.D. is supported by the ARC Future Fellowship Scheme (No. FT150100408). This work was enabled by the use of the Central Analytical Research Facility hosted by the Institute for Future Environments at QUT. J.F.R.V.G., A.P., and R.H. gratefully acknowledge FWO Flanders and Ghent University for financial support.

DATA AVAILABILITY

The data that support the findings of this study are available within the article and its supplementary material.

REFERENCES

[1]T. R. Dargaville, J. R. Park, and R. Hoogenboom, Macromol. Biosci. **18**, 1800070 (2018).
[2]M. Hartlieb, D. Pretzel, K. Kempe, C. Fritzsche, R. M. Paulus, M. Gottschaldt, and U. S. Schubert, Soft Matter **9**, 4693 (2013).
[3]J.-R. Park, J. F. Van Guyse, A. Podevyn, E. C. Bolle, N. Bock, E. Linde, M. Celina, R. Hoogenboom, and T. R. Dargaville, Eur. Polym. J. **120**, 109217 (2019).
[4]K. Lava, B. Verbraeken, and R. Hoogenboom, Eur. Polym. J. **65**, 98 (2015).
[5]O. Sedlacek, B. D. Monnery, S. K. Filippov, R. Hoogenboom, and M. Hruby, Macromol. Rapid Commun. **33**, 1648 (2012).
[6]O. Sedlacek and R. Hoogenboom, Adv. Ther. **3**, 1900168 (2020).
[7]M. Glassner, K. Lava, V. R. de la Rosa, and R. Hoogenboom, J. Polym. Sci. A Polym. Chem. **52**, 3118 (2014).
[8]M. Glassner, M. Vergaelen, and R. Hoogenboom, Polym. Int. **67**, 32 (2018).
[9]A. B. Cook, R. Peltier, J. Zhang, P. Gurnani, J. Tanaka, J. A. Burns, R. Dallmann, M. Hartlieb, and S. Perrier, Polym. Chem. **10**, 1202 (2019).

[10]S. Cesana, J. Auernheimer, R. Jordan, H. Kessler, and O. Nuyken, Macromol. Chem. Phys. **207**, 183 (2006).
[11]T. R. Dargaville, K. Lava, B. Verbraeken, and R. Hoogenboom, Macromolecules **49**, 4774 (2016).
[12]T. Wloka, S. Czich, M. Kleinsteuber, E. Moek, C. Weber, M. Gottschaldt, K. Liefeith, and U. S. Schubert, Eur. Polym. J. **122**, 109295 (2020).
[13]O. I. Kalaoglu-Altan, Y. Li, R. McMaster, A. Shaw, Z. Hou, M. Vergaelen, R. Hoogenboom, T. R. Dargaville, and K. De Clerck, Eur. Polym. J. **120**, 109218 (2019).
[14]O. Berberich, J. Blöhbaum, S. Hölscher-Doht, R. H. Meffert, J. Teßmar, T. Blunk, and J. Groll, J. Ind. Eng. Chem. **80**, 757 (2019).
[15]R. Luxenhofer and R. Jordan, Macromolecules **39**, 3509 (2006).
[16]Y. Jiang, J. Chen, C. Deng, E. J. Suuronen, and Z. Zhong, Biomaterials **35**, 4969 (2014).
[17]A. M. Kelly and F. Wiesbrock, Macromol. Rapid Commun. **33**, 1632 (2012).
[18]Y. Chujo, K. Sada, and T. Saegusa, Macromolecules **23**, 2636 (1990).
[19]T. Li, H. Tang, and P. Wu, Soft Matter **11**, 1911 (2015).
[20]A. P. Mathew, S. Uthaman, K.-H. Cho, C.-S. Cho, and I.-K. Park, Int. J. Biol. Macromol. **110**, 17 (2018).
[21]A. S. Carlini, R. Gaetani, R. L. Braden, C. Luo, K. L. Christman, and N. C. Gianneschi, Nat. Commun. **10**, 1 (2019).
[22]B. D. Monnery and R. Hoogenboom, Polym. Chem. **10**, 3480 (2019).
[23]M. M. Lübtow, T. Lorson, T. Finger, F. K. Gröber-Becker, and R. Luxenhofer, Macromol. Chem. Phys. **221**, 1900341 (2019).
[24]S. Kirchhof, F. P. Brandl, N. Hammer, and A. M. Goepferich, J. Mater. Chem. B **1**, 4855 (2013).
[25]C. García-Astrain, A. Gandini, D. Coelho, I. Mondragon, A. Retegi, A. Eceiza, M. Corcuera, and N. Gabilondo, Eur. Polym. J. **49**, 3998 (2013).
[26]H. Wang, D. Zhu, A. Paul, L. Cai, A. Enejder, F. Yang, and S. C. Heilshorn, Adv. Funct. Mater. **27**, 1605609 (2017).
[27]Z. Zhang, C. He, and X. Chen, Mater. Chem. Front. **2**, 1765 (2018).
[28]P. Šedová *et al.*, Carbohydr. Polym. **216**, 63 (2019).
[29]F. Yu, X. Cao, Y. Li, L. Zeng, B. Yuan, and X. Chen, Polym. Chem. **5**, 1082 (2013).
[30]J. Su, Gels **4**, 72 (2018).
[31]V. Crescenzi, L. Cornelio, C. Di Meo, S. Nardecchia, and R. Lamanna, Biomacromolecules **8**, 1844 (2007).
[32]M. Lutolf and J. Hubbell, Biomacromolecules **4**, 713 (2003).
[33]C. M. Nimmo and M. S. Shoichet, Bioconjugate Chem. **22**, 2199 (2011).
[34]W. Yan, M. Divandari, J.-G. Rosenboom, S. N. Ramakrishna, L. Trachsel, N. D. Spencer, G. Morgese, and E. M. Benetti, Polym. Chem. **9**, 2580 (2018).
[35]Y.-S. Hwang, P.-R. Chiang, W.-H. Hong, C.-C. Chiao, I.-M. Chu, G.-H. Hsiue, and C.-R. Shen, PLoS One **8**, e67495 (2013).
[36]E. Rossegger, V. Schenk, and F. Wiesbrock, Polymers **5**, 956 (2013).
[37]R. W. Moreadith *et al.*, Eur. Polym. J. **88**, 524 (2017).
[38]S. M. Hodgson, E. Bakaic, S. A. Stewart, T. Hoare, and A. Adronov, Biomacromolecules **17**, 1093 (2016).
[39]S. M. Hodgson, S. A. McNelles, L. Abdullahu, I. A. Marozas, K. S. Anseth, and A. Adronov, Biomacromolecules **18**, 4054 (2017).
[40]N. J. Agard, J. A. Prescher, and C. R. Bertozzi, J. Am. Chem. Soc. **126**, 15046 (2004).
[41]A. D. Kent, N. G. Spiropulos, and J. M. Heemstra, Anal. Chem. **85**, 9916 (2013).
[42]E. Kim and H. Koo, Chem. Sci. **10**, 7835 (2019).
[43]H. Jiang, S. Qin, H. Dong, Q. Lei, X. Su, R. Zhuo, and Z. Zhong, Soft Matter **11**, 6029 (2015).
[44]S. Fu, H. Dong, X. Deng, R. Zhuo, and Z. Zhong, Carbohydr. Polym. **169**, 332 (2017).
[45]C. M. Madl, L. M. Katz, and S. C. Heilshorn, Adv. Funct. Mater. **26**, 3612 (2016).
[46]J. F. Van Guyse, M. A. Mees, M. Vergaelen, M. Baert, B. Verbraeken, P. J. Martens, and R. Hoogenboom, Polym. Chem. **10**, 954 (2019).
[47]Y. Xie, S. C. Rizzi, R. Dawson, E. Lynam, S. Richards, D. I. Leavesley, and Z. Upton, Tissue Eng. Part C Methods **16**, 1111 (2010).
[48]P. Haridas, J. A. McGovern, A. S. Kashyap, D. S. McElwain, and M. J. Simpson, Sci. Rep. **6**, 1 (2016).
[49]P. J. Bouten, D. Hertsen, M. Vergaelen, B. D. Monnery, S. Catak, J. C. van Hest, V. Van Speybroeck, and R. Hoogenboom, J. Polym. Sci. A Polym. Chem. **53**, 2649 (2015).
[50]J.-R. Park, M. Sarwat, E. C. Bolle, M. A. de Laat, J. F. Van Guyse, A. Podevyn, R. Hoogenboom, and T. R. Dargaville, Polym. Chem. **11**, 5191 (2020).
[51]M. Cegłowski and R. Hoogenboom, Macromolecules **51**, 6468 (2018).
[52]M. Burk, S. Rothstein, and P. Dubé, Org. Process Res. Dev. **22**, 108 (2018).
[53]B. Reux, V. Weber, M.-J. Galmier, M. Borel, M. Madesclaire, J.-C. Madelmont, E. Debiton, and P. Coudert, Bioorg. Med. Chem. **16**, 5004 (2008).
[54]P. V. Chang, J. A. Prescher, E. M. Sletten, J. M. Baskin, I. A. Miller, N. J. Agard, A. Lo, and C. R. Bertozzi, Proc. Natl. Acad. Sci. U.S.A. **107**, 1821 (2010).
[55]P. Ostrovskis, C. M. R. Volla, M. Turks, and D. Markovic, Curr. Org. Chem. **17**, 610 (2013).
[56]K. S. Anseth, C. N. Bowman, and L. Brannon-Peppas, Biomaterials **17**, 1647 (1996).
[57]S. Choi, E. Y. Choi, D. J. Kim, J. H. Kim, T. S. Kim, and S. W. Oh, Clin. Chim. Acta **339**, 147 (2004).
[58]Y. Bernhard, O. Sedlacek, J. F. Van Guyse, J. Bender, Z. Zhong, B. G. De Geest, and R. Hoogenboom, Biomacromolecules **21**, 3207 (2020).
[59]M. Koitka, J. Höchel, H. Gieschen, and H.-H. Borchert, J. Pharm. Biomed. Anal. **51**, 664 (2010).
[60]J. K. Sodhi, S. Wong, D. S. Kirkpatrick, L. Liu, S. C. Khojasteh, C. E. Hop, J. T. Barr, J. P. Jones, and J. S. Halladay, Drug Metab. Dispos. **43**, 908 (2015).
[61]See the supplementary material at https://doi.org/10.1116/6.0000630 for synthesis routes and characterizations of 4-azidobutanoic acid and cyclooct-1-yn-3-glycolic acid (NMR and MS); synthesis route of C3MestOx monomer; characterizations of polymers (IR); rheological properties of hydrogels.